Journal of Engineering Mathematics **50:** 241–266, 2004.

Surface-tension-driven dewetting of Newtonian and power-law fluids

J.C. FLITTON and J.R. KING
Theoretical Mechanics Section, School of Mathematical Sciences, University of Nottingham, Nottingham NG7 2RD, UK

Received 1 December 2003; accepted in revised form 15 July 2005

Abstract. The dewetting over a planar substrate of a thin layer of highly viscous fluid under the action of surface tension is considered, with a doubly-nonlinear fourth-order degenerate parabolic equation governing the flow of a power-law fluid. Asymptotic methods are applied to analyse the motion in the shear-thinning, shear-thickening and Newtonian cases, the last of these corresponding mathematically to a critical value of the relevant exponent. In particular, the role played by the local behaviour in the neighbourhood of the contact line is analysed and the dependence of the one-dimensional large-time dewetting behaviour on the fluid's constitutive properties characterised. Stability issues are also touched upon.

Key words: contact-line motion, high-order nonlinear diffusion, shear-thinning and shear-thickening fluids, thin-film flows

1. Introduction

When the motion over a planar substrate of a thin film of a fluid with a shear-dependent power-law viscosity is controlled by a balance between viscosity and surface tension, the surface height profile can be taken to be governed by the (suitable scaled) evolution equation

$$\frac{\partial h}{\partial t} = \nabla \cdot \left(h^n \, |\nabla p|^{m-1} \, \nabla p \right), \quad p = -\nabla^2 h, \tag{1}$$

where h is the height of the fluid layer, p is the pressure and n and m are positive constants. In what follows we can, in the main, limit the discussion to the one-dimensional form of this system, *i.e.*,

$$\frac{\partial h}{\partial t} = -\frac{\partial}{\partial x} \left(h^n \left| \frac{\partial^3 h}{\partial x^3} \right|^{m-1} \frac{\partial^3 h}{\partial x^3} \right). \tag{2}$$

A full derivation is given by King [1], the formulation (1) arising as the appropriate lubrication limit when the fluid viscosity takes the form

$$\mu = \mu_0 (2 d_{ij} d_{ij})^{\frac{1-m}{2m}}$$

where μ_0 is a constant and

$$d_{ij} = \tfrac{1}{2} \left(\frac{\partial u_i}{\partial x_j} + \frac{\partial u_j}{\partial x_i} \right)$$

is the rate-of-strain tensor, the velocity vector being (u_1, u_2, u_3) in Cartesian coordinates (x_1, x_2, x_3). The exponents n and m in (2) are related for a power-law fluid by $n = m + 2$; a Newtonian fluid has $m = 1$, $n = 3$, this case representing the borderline between shear-thinning, $m > 1$, and shear-thickening, $m < 1$, fluids and corresponding mathematically to a critical

exponent (see below). In much of what follows, however, we treat (at very little additional algebraic cost) n and m as independent.

The behaviour naturally depends both on the fluid properties (*i.e.*, on m) and on the contact-line dynamics, the latter being expressed in terms of a moving-boundary (contact angle) condition. The prescription of such a condition remains a matter of controversy, with the relationship between "macroscopic" and "microscopic" contact angles being a key issue; see [2–4], for instance.

Analysis of fluids with shear-dependent viscosity has previously been carried out in [5–8], for example, in the contexts of droplet spreading and film drainage. Other applications of thin-film modelling of power-law fluids include rivulet flows [9]. The current work, however, focuses on dewetting flows, which have been the subject of markedly less analysis. Existing studies postulate a number of different behaviours for the time-dependence of the dewetting radius. For example, [10] considered the dependence on the constitutive assumption for the viscosity and on the initial film thickness, power-law time dependencies being most prevalent, but with exponential growth being suggested at early times. The analysis in [11] and [12] leads to linear dependence on t for Newtonian fluids, the latter also suggesting linear growth for power-law fluids. Our analysis is concerned with cases in which a dry region has already been initiated; unlike many previous studies (*e.g.* [13–15]) we do not therefore incorporate van der Waals forces in investigating film rupture.

Experimental analysis of dewetting has focused particularly on thin-film polymers, for which the viscosity is often assumed to be shear-dependent. In particular, [16] considered polymer films for which the dewetting radius was found to grow exponentially for small time, followed by a period of linear growth (the width of the "rim" of fluid was found to grow as $t^{1/2}$, consistent with [12] and with the analysis below), before a final regime in which the dewetting radius goes like $t^{2/3}$; in addition, [16–18] found the dewetting radius to grow linearly for a variety of Newtonian fluids. The role of inertia in high-speed dewetting is discussed in [19]. The mechanisms used to initiate dewetting by forcing touch-down often cause more than one dewetting region to be created. When the resulting dry zones become sufficiently large they of course interact, preventing idealised asymptotic behaviour being realised. This has been considered by [20,21], for instance, where the pattern formation of dewetting fluids has been examined (see also [22] for relevant observations in a slightly different context); we shall not consider such matters here. Experimental studies have also identified instabilities at the receding edge [23,24]. Finally, we note that issues related to those which we consider here arise in studies of crater formation in paint drying; see [25] for example.

The paper is organised as follows. We first consider "shear-thinning" fluids, for which $n < 2m+1$, followed by "shear-thickening" ones. Newtonian fluids, $m=3$, $n=1$ are then considered, before we discuss the results in Section 5. We focus primarily on the one-dimensional case, though the results carry over readily to cylindrical symmetry; we also undertake a preliminary investigation of multi-dimensional stability issues, with much more remaining to be done in this regard. We remark here that the discussion (Section 5) includes a summary of our results and as such may provide a useful guide to what follows.

2. "Shear-thinning" fluids; $n < 2m+1$

2.1. Problem formulation

The "shear-thinning" regime corresponds (for reasons described in [6] and implicit in the analysis below) to $n < 2m+1$, so for power-law fluids (*i.e.*, for $n = m+2$) we have $m > 1$. We

assume that a thin layer of fluid, of infinite extent, lies over on a horizontal substrate such that

$$h(\mathbf{x}, 0) = h_i(\mathbf{x})$$

for definiteness, much of the analysis will concentrate on the case $h_i = 1$ away from some neighbourhood of the origin. The fluid layer dewets from the point $\mathbf{x} = \mathbf{0}$ at which it touches down (or where the interface is initially located if a finite dry patch is present from the start). At the receding contact line the fluid height is zero and the contact angle is positive and will be assumed, for simplicity, to be constant. We note that the analysis can be generalised to non-constant contact angles and that the analysis of [6] shows that for shear-thinning fluids the "macroscopic" contact angle can be identified with the "microscopic" one. Thus the evolution Equation (2) can be applied as it stands in the shear-thinning case; in the Newtonian and shear-thickening cases we shall need to include additional regularising terms in order to allow interface motion (*cf.* [5,6]).

In planar geometry, we write the interface as $x = s(t)$ with $s(0) = 0$, and we set as our moving boundary conditions

$$h = 0, \quad \frac{\partial h}{\partial x} = \lambda, \qquad h^n \left| \frac{\partial^3 h}{\partial x^3} \right|^{m-1} \frac{\partial^3 h}{\partial x^3} = 0 \quad \text{at } x = s(t), \tag{3}$$

the contact angle is thus denoted by λ and there is zero mass flux through the contact line. No flow occurs as $x \to \infty$, so we have

$$h \to 1 \quad \text{as } x \to +\infty,$$

since we scale such that $h_i \to 1$ as $x \to +\infty$. For large time the height of the film somewhat ahead of the receding edge is much greater than that of the initial configuration. Figure 1 shows a schematic of the dewetting process for early and late times; for brevity our analysis describes only the fluid region in $x > 0$.

2.2. Small-time behaviour

We now describe the small-time behaviour of (2–3) with $n < 2m + 1$, in particular because this provides useful insight into the subsequent evolution. For $x = O(1)$, *i.e.*, away from the contact line near $x = 0$,

$$h \sim h_i(x) - \frac{\mathrm{d}}{\mathrm{d}x} \left(h_i^n \left| \frac{\mathrm{d}^3 h_i}{\mathrm{d}x^3} \right|^{m-1} \frac{\mathrm{d}^3 h_i}{\mathrm{d}x^3} \right) t$$

applies as $t \to 0$. Here we assume that

$$h_i(x) \sim A x^p \quad \text{as } x \to 0^+$$

with $p \geq 1$ (if $p < 1$ then $s(t)$ will initially seek to decrease so, unless there is a finite pre-existing dry region, the film will lift back up again). In practice the value of the exponent p will be determined by the behaviour as the film initially touches down, an issue of interest in its own right. For $p = 1$ we postulate a small-time similarity solution of the form

$$h(x, t) \sim t^{\frac{1}{2m+2-n}} f\left(x / t^{\frac{1}{2m+2-n}} \right), \qquad s(t) \sim \eta_0 t^{\frac{1}{2m+2-n}} \tag{4}$$

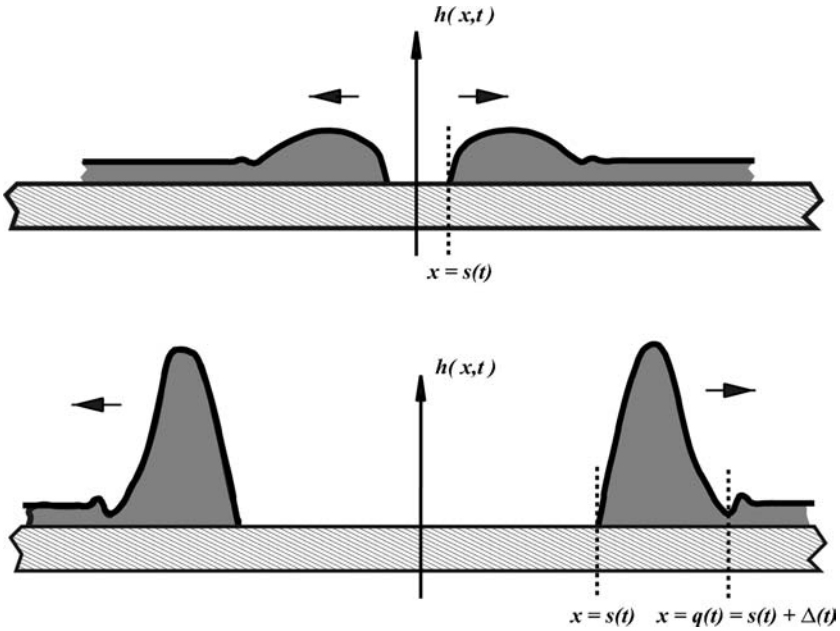

Figure 1. The dewetting process. A thin layer of fluid is forced to touch down. The dry region then expands and a ridge forms behind the receding edge. At large time the height of this ridge is significantly larger than that of the undisturbed layer.

with $f(\eta) \sim A\eta$ as $\eta \to \infty$. It follows that $f(\eta) = \lambda\eta$, $\eta_0 = 0$ for $A = \lambda$ and we expect $\eta_0 > 0$ for $0 < A < \lambda$ (with $\eta_0 < 0$ for $A > \lambda$, so in this case too the extent of any dry region will decrease); since $n < 2m + 1$ this corresponds to sublinear growth of s with t.

For $p > 1$ (and for $p = 1$ with $A \to 0$) the structure is very similar to that arising in the large-time limit and, since the latter is a more significant limit physically, we defer detailed description to Section 2.3. In summary, however, we have a "hump" (or "rim") of fluid immediately to the right of the contact line with, setting $x = s(t) + z$, leading-order balance

$$\begin{aligned} &\dot{s} = h^{n-1}\left|\frac{\partial^3 h}{\partial z^3}\right|^{m-1}\frac{\partial^3 h}{\partial z^3}, \\ &h = 0, \quad \frac{\partial h}{\partial z} = \lambda \text{ at } z = 0, \\ &h = 0, \quad \frac{\partial h}{\partial z} = 0 \text{ at } z = \Delta(t), \end{aligned} \tag{5}$$

subject to (for conservation of mass, given that $\Delta \ll s$)

$$\int_0^{\Delta(t)} h \, \mathrm{d}z = \frac{As^{p+1}}{p+1}, \tag{6}$$

giving a formulation from which both s and Δ must be determined; the boundary conditions on $z = \Delta$ follow from a matching argument given in Section 2.3.2. Since the boundary-value problem (5) is analysed in some detail below, for the time being we need only note that scaling arguments imply that

$$h(z,t) = \lambda^{\frac{3m}{2m+1-n}}\dot{s}^{-\frac{1}{2m+1-n}}\bar{h}(\zeta), \qquad z = \lambda^{\frac{m-1+n}{2m+1-n}}\dot{s}^{-\frac{1}{2m+1-n}}\zeta, \qquad \Delta(t) = \zeta_0\lambda^{\frac{m-1+n}{2m+1-n}}\dot{s}^{-\frac{1}{2m+1-n}} \tag{7}$$

for some constant $\zeta_0(n,m)$ which is determined as part of the solution to

$$\begin{aligned}
&\bar{h}^{\frac{n-1}{m}}\frac{\mathrm{d}^3\bar{h}}{\mathrm{d}\zeta^3}=1,\\
&\bar{h}=0,\quad \frac{\mathrm{d}\bar{h}}{\mathrm{d}\zeta}=1 \text{ at } \zeta=0,\\
&\bar{h}=0,\quad \frac{\mathrm{d}\bar{h}}{\mathrm{d}\zeta}=0 \text{ at } \zeta=\zeta_0,;
\end{aligned} \tag{8}$$

it is easily seen that $\mathrm{d}^3\bar{h}/\mathrm{d}\zeta^3$ is strictly positive for $\zeta\in(0,\zeta_0)$. From (6) we then obtain that

$$M\lambda^{\frac{4m-1+n}{2m+1-n}}\dot{s}^{-\frac{2}{2m+1-n}}\sim\frac{As^{p+1}}{p+1}\quad \text{as } t\to 0, \tag{9}$$

where the constant $M(n,m)$, defined by

$$M=\int_0^{\zeta_0}\bar{h}(\zeta)\mathrm{d}\zeta, \tag{10}$$

is determined by the boundary-value problem (8), being proportional to the mass in the fluid hump. Thus

$$s\sim s_0 t^{\frac{2}{(2m+1-n)(p+1)+2}}\quad \text{as } t\to 0, \tag{11}$$

again representing sublinear growth, where the positive constant s_0 is given by

$$s_0=\left(\frac{(2m+1-n)(p+1)+2}{2}\right)^{\frac{2}{(2m+1-n)(p+1)+2}}\left(\frac{(p+1)M}{A}\right)^{\frac{2m+1-n}{(2m+1-n)(p+1)+2}}\lambda^{\frac{4m-1+n}{(2m+1-n)(p+1)+2}}. \tag{12}$$

2.3. Large-time behaviour

2.3.1. *Outer Solution*

2.3.1.1. *Time dependence* This section is concerned with the limit $t\to\infty$. We first characterise the evolution in terms of the power laws which arise in the time dependence and then describe in more detail the spatial profiles in the various regions that make up the fluid film, referring to Figure 3 for schematic of the corresponding asymptotic structure. We again choose a frame of reference moving with the dewetting boundary, giving (with $x=s(t)+z$)

$$\frac{\partial h}{\partial t}-\dot{s}\frac{\partial h}{\partial z}=-\frac{\partial}{\partial z}\left(h^n\left|\frac{\partial^3 h}{\partial z^3}\right|^{m-1}\frac{\partial^3 h}{\partial z^3}\right). \tag{13}$$

As the contact line moves a dry region is formed, the fluid that once lay in this region being swept up into a hump ahead of the contact line. We denote the width of this rim (defined more precisely shortly) by $\Delta(t)$ and note that the fluid layer is almost undisturbed for $x>q(t)$, where $q=s+\Delta$. Conservation of mass then implies (in planar geometry) that, in our large time analysis,

$$\int_{s(t)}^{q(t)}h(x,t)\mathrm{d}x\sim\int_0^{q(t)}h_i(x)\mathrm{d}x. \tag{14}$$

We shall find that $\Delta/s \to 0$ as $t \to \infty$, so to leading order (14) becomes

$$\int_0^{\Delta(t)} h(z,t)\mathrm{d}z \sim s(t) \tag{15}$$

(this approximation to the right-hand side of (14) follows because $h_i \sim 1$ for large x and $q \sim s \gg 1$ for large t). The dominant large-time balance in (13) is quasi-steady so, using (3), we recover (5) to leading order (the conditions on $z = \Delta(t)$ will be derived shortly by matching into the inner region); one relation between Δ and s is determined by (15) and the second by (5). It again follows from a scaling argument that the solution to (5) takes the form (7) (we shall see shortly that $\dot{s} \to 0$ as $t \to \infty$), with $\bar{h}$ given by (8). The location of the interface can then be determined from (15), giving (*cf.* (9))

$$M\lambda^{\frac{4m-1+n}{2m+1-n}}\dot{s}^{-\frac{2}{2m+1-n}} \sim s \quad \text{as } t \to \infty. \tag{16}$$

From (16) we have

$$s \sim \left(\frac{2m+3-n}{2}\right)^{\frac{2}{2m+3-n}} M^{\frac{2m+1-n}{2m+3-n}}\lambda^{\frac{4m-1+n}{2m+3-n}}t^{\frac{2}{2m+3-n}} \quad \text{as } t \to \infty, \tag{17}$$

and from (7) it then follows that h, $\Delta \propto t^{1/(2m+3-n)}$ as $t \to \infty$ and the self-consistency requirement that $\Delta \ll s$ as $t \to \infty$ is necessarily satisfied. In the *bona fide* power-law fluid case $n = m+2$ we thus have

$$\begin{aligned} s &\sim \left(\frac{m+1}{2}\right)^{\frac{2}{m+1}} M^{\frac{m-1}{m+1}}\lambda^{\frac{5m+1}{m+1}}t^{\frac{2}{m+1}}, \\ \Delta &\sim \zeta_0\left(\frac{m+1}{2}\right)^{\frac{1}{m+1}} \lambda^{-\frac{(2m+1)(5m+1)}{(m+1)(m-1)^2}} M^{-\frac{1}{m+1}}t^{\frac{1}{m+1}} \quad \text{as } t \to \infty. \end{aligned} \tag{18}$$

Moreover, in the Navier-slip dominated case $n = 2$, $m = 1$, which also lies in this regime, we have

$$s \sim \left(\frac{3}{2}\right)^{\frac{2}{3}} M^{\frac{1}{3}}\lambda^{\frac{5}{3}}t^{\frac{2}{3}}, \qquad \Delta \sim \zeta_0\left(\frac{3}{2}\right)^{\frac{1}{3}} M^{-\frac{1}{3}}\lambda^{\frac{1}{3}}t^{\frac{1}{3}}, \tag{19}$$

the $t^{2/3}$ power-law having been noted elsewhere (*e.g.* [26], in which the rim profile is also analysed, [11], [16] and [27]). In the limit $n \to (2m+1)^-$ in which the borderline is approached we have $s \propto t$ and $\Delta \propto t^{1/2}$, allowing a smooth transition in time dependence to the results of the subsequent sections.

2.3.1.2. *Rim profile* The boundary-value problem (8) is readily solved in the special cases $n = 1$ (corresponding to a shear thinning fluid in a Hele-Shaw cell; see [1]), in which

$$\bar{h} = \zeta\left(1 - \frac{1}{\sqrt{6}}\zeta\right)^2, \quad \zeta_0 = \sqrt{6}, \quad M = \frac{1}{2},$$

and $n = 1 - m$ (so that (8) is linear), which we do not detail because it is not pertinent to power-law fluids. For $n = m+1$ (which includes the slip-dominated case $n = 2$, $m = 1$ and, in effect, the very shear-thinning limit $n = m+2$ with $m \to \infty$) a first integral is available, whereby

$$\bar{h}\frac{\mathrm{d}^2\bar{h}}{\mathrm{d}\zeta^2} - \frac{1}{2}\left(\frac{\mathrm{d}\bar{h}}{\mathrm{d}\zeta}\right)^2 = \zeta - \frac{1}{2}$$

so that $\zeta_0 = 1/2$. Finally, the limit $n \to (2m+1)^-$ in which the borderline is approached is worth analysing both because of what will follow in later sections and in view of its intrinsic asymptotic interest. We set $n = 2m+1-\nu m$ with $0 < \nu \ll 1$, so that

$$\bar{h}^{2-\nu} \frac{\mathrm{d}^3 \bar{h}}{\mathrm{d}\zeta^3} = 1. \tag{20}$$

There are two exponentially narrow inner regions. In the left-hand one ($\xi_L = O(1)$, ζ exponentially small in ν) we set

$$\bar{h} = \zeta \, \Phi_L(\xi_L), \qquad \xi_L = \nu \log \zeta + \log(1/\nu)$$

with leading-order problem

$$\mathrm{e}^{-\xi_L} \Phi_L^2 \frac{\mathrm{d}\Phi_L}{\mathrm{d}\xi_L} \sim -1, \quad \Phi_L \to 1 \text{ as } \xi_L \to -\infty$$

so that

$$\Phi_L \sim \left(1 - 3\mathrm{e}^{\xi_L}\right)^{\frac{1}{3}}. \tag{21}$$

Similarly, in the right-hand one (for $\xi_R = O(1)$, $\zeta_0 - \zeta$ exponentially small) we set

$$\bar{h} = (\zeta_0 - \zeta) \, \Phi_R(\xi_R), \qquad \xi_R = -\nu \log(\zeta_0 - \zeta) - \log(1/\nu)$$

to give

$$\mathrm{e}^{\xi_R} \Phi_R^2 \frac{\mathrm{d}\Phi_R}{\mathrm{d}\xi_R} \sim -1, \qquad \Phi_R \to 0 \text{ as } \xi_R \to +\infty$$

and hence

$$\Phi_L \sim 3^{\frac{1}{3}} \mathrm{e}^{-\xi_R/3}. \tag{22}$$

The outer region has ζ, $\bar{h} = O(\zeta_0)$, where ζ_0 will itself prove to be exponentially small in ν (the inner regions are in fact exponentially smaller than ζ_0); hence the dominant balance there is quasi-steady (*i.e.*, the left-hand side of (20) is negligible), implying

$$\bar{h} \sim \Lambda_0 \zeta \, (\zeta_0 - \zeta) / \zeta_0, \tag{23}$$

where the constant $\Lambda_0 = O(1)$ remains to be determined. Matching with (21),(22), with the outer scaling $\zeta = O(\zeta_0)$ corresponding to $\xi_L \sim \nu \log \zeta_0 + \log(1/\nu)$, $\xi_R \sim -\nu \log \zeta_0 - \log(1/\nu)$, yields

$$\Lambda_0 \sim \left(1 - \frac{3\zeta_0^\nu}{\nu}\right)^{\frac{1}{3}} \sim \left(\frac{3\zeta_0^\nu}{\nu}\right)^{\frac{1}{3}}$$

so that

$$\Lambda_0 = 2^{-\frac{1}{3}}, \qquad \nu \log \zeta_0 \sim -\log(1/\nu) - \log 6, \quad \text{as } \nu \to 0$$

so ζ_0 behaves essentially as $(\nu/6)^{1/\nu}$ for small ν, this very rapid decay with decreasing ν being very striking. Moreover the macroscopic contact angle (corresponding to Λ_0) is a factor $2^{-1/3}$ smaller than the microscopic one.

We now outline our numerical solution procedure for obtaining solutions to (8) for arbitrary $n < 2m+1$. We use the local behaviour near to $z=0$, whereby the first three terms in the local expansion read (for $n \neq m+1$)

$$\bar{h} \sim \zeta - B\zeta^2 + \frac{m^3}{(m+1-n)(2m+1-n)(3m+1-n)} \zeta^{\frac{3m+1-n}{m}} \quad \text{as } \zeta \to 0 \tag{24}$$

the third term in fact being larger than the second if $n > m+1$. Here B is an arbitrary constant (necessarily positive if $n < m+1$) which we use as our shooting parameter. At the right-hand end we have, as $\zeta \to \zeta_0^-$,

$$\bar{h} \sim A(\zeta_0 - \zeta)^2 \quad \text{for } 2n < m+2, \tag{25}$$

$$\bar{h} \sim \left(\frac{(n+m-1)^3}{3m(2m+1-n)(2n-m-2)} \right)^{\frac{m}{n+m-1}} (\zeta_0 - \zeta)^{\frac{3m}{n+m-1}} \quad \text{for } 2n > m+2, \tag{26}$$

where A is an arbitrary constant; power-law fluids, $n = m+2$, necessarily lie in the regime (26). There are two degrees of freedom at the right-hand end, namely ζ_0 and A for $2n < m+2$ and ζ_0 and the second (power-law) term in the local expansion for $2n > m+2$. Our shooting procedure varies B, starting the solution from a small positive value of ζ, typically 0·01, (with $\bar{h}$ and its first and second derivatives approximated there by (24)) until $\bar{h}$ and $\mathrm{d}\bar{h}/\mathrm{d}\zeta$ are simultaneously zero at some positive ζ; numerical solutions obtained in this way, using NAG routine D02MVF, are shown in Figure 2. It is worth noting that a naive application of the code in the "shear-thickening" regime $n > 2m+1$ fails to generate solutions which touch down; the reasons for this are implicit in the analysis below. We also note that in the capillary-quasi-static limit in which the parabolic profile (23) pertains the rim is symmetric (as we shall see, the same profile arises in the Newtonian and shear-thickening cases). In the shear-thinning case with ν not small, however, the rim profile does not have such a simple "universal" shape, depending on m via (8); this provides a means by which information about the fluid's properties can be inferred directly from the rim profile, in a manner reminiscent of the application of the Boltzmann–Matano method used to extract nonlinear diffusivities from experimental profiles. Thus, under the assumptions described in [1], if the dependence of the viscosity on the strain rate is taken to be more general than power law then the first of (1) (with $n = m+2$) generalises to

$$\frac{\partial h}{\partial t} = \nabla \cdot \left(h^3 D\left(h\,|\nabla p|\right) \nabla p \right),$$

with $D(\phi) = \Lambda(\phi)/\phi^3$ in the notation of [1], wherein a description is given of how Λ is related to the fluid viscosity for the class of constitutive laws with which we are concerned. The first of (1) similarly generalises to

$$\dot{s} = h^3 D\left(h \left| \frac{\partial^3 h}{\partial z^3} \right| \right) \frac{\partial^3 h}{\partial z^3}, \tag{27}$$

so by measuring the dependence of the rim profile h on z it is in principle possible to deduce $D(\phi)$, and hence the dependence of the viscosity on the strain rate, via

$$D(\phi) = \dot{s}/h^2\phi, \quad \phi = h\frac{\partial^3 h}{\partial z^3}.$$

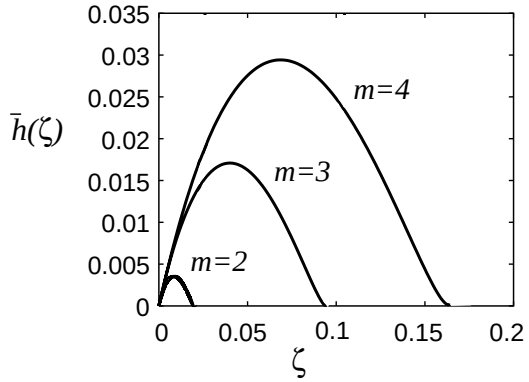

Figure 2. Plot of the "travelling-wave" solution for the rim of dewetting fluid. In these plots $n=m+2$ (corresponding to a shear-thinning fluid) and $m=2$, 3 and 4, the size of the hump increasing as m increases (we note that $v=1-1/m$ for $n=m+2$, so that $m=2$ corresponds to $v=1/2$).

However, since $\phi=O(1/\Delta)$ as $t\to\infty$, this approach will only identify the behaviour for small shear rates unless care is taken to ensure that an intermediate asymptotic regime exists over which the full balance applies in (27), before the flow evolves for large times according to the small ϕ limit of $D(\phi)$.

2.3.2. *Inner solution ahead of hump*

To specify the asymptotic structure fully and to justify the above boundary conditions at $z=\Delta(t)$ we must match from the outer 'hump' into the undisturbed layer ahead. We now translate to the front of the hump, setting

$$x=q(t)+\hat{z}.$$

Since $q\sim s$ as $t\to\infty$ and we require $h\to 1$ as $\hat{z}\to+\infty$ we have at leading order that

$$\dot{s}(h-1)=h^n\left|\frac{\partial^3 h}{\partial\hat{z}^3}\right|^{m-1}\frac{\partial^3 h}{\partial\hat{z}^3}. \tag{28}$$

We restrict ourselves for brevity to the range $2n>m+2$ in which (26) provides the matching condition as $\hat{z}\to-\infty$. This encompasses the slip-dominated case $n=2, m=1$, as well as shear-thinning fluids $n=m+2$. For an analysis of other ranges in the case $m=1$ (such results readily generalise) in a slightly different context see [28]; for given m, film rupture is possible for sufficiently small n, in which case the material which becomes disconnected from the rest of the film will bunch up into a parabolic (steady-state) profile and the process can then repeat, with a sequence of "droplets" left behind. For $2n>m+2$ we have the leading-order problem

$$\begin{aligned}
&h-1=h^n\left|\frac{\mathrm{d}^3 h}{\mathrm{d}\hat{\zeta}^3}\right|^{m-1}\frac{\mathrm{d}^3 h}{\mathrm{d}\hat{\zeta}^3},\\
&h\sim\left(\frac{(n+m-1)^3}{3m(2m+1-n)(2n-m-2)}\right)^{\frac{3m}{n+m-1}}\left(-\hat{\zeta}\right)^{\frac{3m}{n+m-1}}\quad\text{as }\hat{\zeta}\to-\infty,\\
&h\to 1\quad\text{as }\hat{\zeta}\to+\infty,
\end{aligned} \tag{29}$$

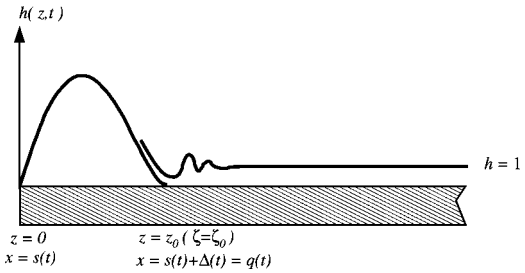

Figure 3. Schematic of inner and outer solutions for a shear-thinning fluid.

where $\hat{z} = \dot{s}^{-1/3m}\hat{\zeta}$ (so $\hat{\zeta} = O(1)$ represents a much narrower region than $\zeta = O(1)$ as $t \to \infty$, as required), which determines h up to translations in $\hat{\zeta}$. A schematic of the matching is given in Figure 3, with the solution decaying to unity in an oscillatory fashion (resulting in the capillary ripples illustrated there); h is not rescaled in (29), so its leading-order minimum value is independent of t (we can specify $q(t)$ precisely by defining it to be the location of this minimum); true rupture cannot occur in the regime $2n > m + 2$ (*i.e.*, h cannot develop an interior zero) within the current modelling framework, but if this minimum is sufficiently small that van der Waals forces (say) are non-negligible then rupture may in fact ensue (*cf.* [14,15], for instance, for the Newtonian case) and a sequence of droplets may be left behind (as in the scenario noted above; *cf.* [29], for example, and see [30] for a discussion of the influence of viscoelastic effects on such behaviour). We note, however, that the minimum thickness is an $O(1)$ multiple (determined by (29)) of the initial film thickness, so van der Waals forces would necessarily also then be non-negligible during the earlier stages of development (*i.e.*, for $t = O(1)$); smaller minimum thicknesses can, however, arise for $t = O(1)$ and their small-time behaviour can be quantified by completing the analysis described in Section 2.2 (whereby $h - 1$ in (29) is replaced by $h - h_i(s)$ in the relevant small-time prescription). Thus, taking $h_i(s) \sim As^p$ for small s and setting

$$h = As^p\hat{h}, \qquad \hat{z} = \left(\dot{s} \Big/ \left(As^p\right)^{n+m-1}\right)^{-1/3m} \hat{\zeta}$$

we recover (29) (with h replaced by $\hat{h}$) and it follows from (11) that the minimum of h behaves as $t^{2p/((2m+1-n)(p+1)+2)}$ for small t, a factor proportional to $t^{(p-1)/((2m+1-n)(p+1)+2)}$ smaller than the maximum height in the rim (it follows from (7) that the latter behaves at $t^{(p+1)/((2m+1-n)(p+1)+2)}$). By taking p sufficiently large, we can make this ratio as low as we wish for given (small) t. It would be worthwhile to investigate such effects further by appropriately generalising the second expression in (2) to include van der Waals forces, which would presumably allow *bona fide* film rupture to occur (the corresponding Newtonian problem has been the subject of extensive investigations, see for example [31,32] and references therein, which it would be interesting to generalise to the case of power-law fluids).

For axisymmetric dewetting the leading-order equations governing the behaviour near the dewetting boundary are identical to those in the analysis above (being locally one-dimensional at leading order), with x replaced by the radial distance r. The only change is that the conservation of mass condition (15) is replaced by

$$2\pi s \int_0^{\Delta(t)} h(z,t)\mathrm{d}z \sim \pi s^2, \tag{30}$$

where $z = r - s(t)$. Consequently we define M_a, the axisymmetric equivalent of M, as

$$M_a = 2\int_0^{\zeta_0} \bar{h}(\zeta)\mathrm{d}\zeta \tag{31}$$

and the analysis otherwise proceeds as before.

3. "Shear-thickening" fluids; $n > 2m + 1$

3.1. Formulation

This section corresponds to the 'fixed front' regime of [1], which encompasses in particular the shear-thickening fluid case $n = m + 2$ with $0 < m < 1$ and the thin-film equation ($m = 1$) with $n > 3$. We would gain little in brevity by restricting attention to these special cases, however, though for reasons which will shortly become clear we shall restrict ourselves to the regime $n < 2m + 2$. Since the unregularised equation does not permit interface motion for finite-contact angle solutions we must introduce a suitable regularisation. The one we adopt corresponds to Navier slip (*cf.* [4] and references therein), this choice being made for illustrative purposes; similar analyses apply for other regularisations but, as noted in [6], can lead to somewhat different behaviour, so that shear-thickening fluids in principle provide a means by which different contact-line physics can readily be distinguished (the situation with Newtonian fluids is more delicate, as we shall see). Again restricting attention for the time being to the one-dimensional case we then have

$$\frac{\partial h}{\partial t} = -\frac{\partial}{\partial x}\left(\left(h^n\left|\frac{\partial^3 h}{\partial x^3}\right|^{m-1} + \epsilon h^2\right)\frac{\partial^3 h}{\partial x^3}\right) \tag{32}$$

with $\epsilon \ll 1$ and

$$h = 0, \quad \frac{\partial h}{\partial x} = \lambda, \quad \left(h^n\left|\frac{\partial^3 h}{\partial x^3}\right|^{m-1} + \epsilon h^2\right)\frac{\partial^3 h}{\partial x^3} = 0 \quad \text{at } x = s(t). \tag{33}$$

In order to describe concisely the way in which the slip condition manifests itself in the macroscopic behaviour it is convenient first to describe in a rather *ad hoc* fashion the behaviour of the interior layer about $x = s(t)$. The scalings of x, s, t and h in the limit $\epsilon \to 0$ depend on circumstances, but the leading-order balance in the cases of interest to us is of travelling wave type, whereby (writing $x = s(t) + z$)

$$\dot{s}h = \left(h^n\left|\frac{\partial^3 h}{\partial z^3}\right|^{m-1} + \epsilon h^2\right)\frac{\partial^3 h}{\partial z^3} \tag{34}$$

to leading order, which is to be solved subject to

$$h = 0, \quad \frac{\partial h}{\partial z} = \lambda \quad \text{at } z = 0 \tag{35}$$

and

$$h \sim \Lambda(t) z \quad \text{as } z \to +\infty \tag{36}$$

where $\Lambda(t)$ is determined as part of the solution ((36) corresponds to the single boundary condition that the solution to (34) contains no z^2 term as $z \to +\infty$). In view of the scaling

properties of (34–36), it follows that

$$h = \left(\frac{\epsilon^m}{|\dot{s}|^{m-1}}\right)^{\frac{1}{n-m-1}} \phi_{\pm}\left(\left(\frac{|\dot{s}|^{n+m-3}}{\epsilon^{n+m-1}}\right)^{\frac{1}{3(n-m-1)}} z; \left(\frac{\epsilon^{n-2m-1}}{|\dot{s}|^{n-2m}}\right)^{\frac{1}{3(n-m-1)}} \lambda\right) \tag{37}$$

for some functions $\phi_{\pm}$ (according to the sign of $\dot{s}$) and hence that

$$\Lambda(t) = \left(\frac{|\dot{s}|^{n-2m}}{\epsilon^{n-2m-1}}\right)^{\frac{1}{3(n-m-1)}} \psi_{\pm}\left(\left(\frac{\epsilon^{n-2m-1}}{|\dot{s}|^{n-2m}}\right)^{\frac{1}{3(n-m-1)}} \lambda\right) \tag{38}$$

for some $\psi_{\pm}$; since the leading-order outer solution is subject to the matching condition $\partial h/\partial x = \Lambda$ at $x = s$, this in turn implies that we should prescribe

$$\frac{\mathrm{d}s}{\mathrm{d}t} = -\epsilon^{\frac{n-2m-1}{n-2m}} \left(\frac{\partial h}{\partial x}\right)^{\frac{3(n-m-1)}{n-2m}} \Psi\left(\lambda \Big/ \frac{\partial h}{\partial x}\right) \quad \text{at } x = s(t), \tag{39}$$

or some limit thereof, on the outer solution. The calculation of the function $\Psi(\mu)$ (whose relationship to $\psi_{\pm}$ is easily identified from (38–39)) requires solution of the boundary-value problem (34–36); key properties of $\Psi(\mu)$ follow from the observation that $h \equiv \lambda z$ when $\dot{s} = 0$, so that $\Psi(1) = 0$, and by noting (34–36) has a solution when $\lambda = 0$ (*i.e.*, the limit $\lambda \to 0^+$ is not a singular one) implying that $\Psi(0) = \kappa_0$ for some positive constant κ_0. The limit $\mu \to +\infty$ is the most important for our purposes. Setting $\Lambda = 0$ in (36), one finds that the far-field balance

$$h \sim C z^{\frac{3m}{m+n-1}} \quad \text{as} \quad z \to +\infty, \tag{40}$$

is possible, with

$$C^{m+n-1} = \left(\frac{(m+n-1)^3}{3m(n-2m-1)(2n-m-2)}\right)^m \dot{s}. \tag{41}$$

The expression (40) represents two boundary conditions, *i.e.*, (34), (35), (40) in effect represents an eigenvalue problem for the second argument of $\phi_{\pm}$ in (37), with a solution only for

$$\left(\frac{\epsilon^{n-2m-1}}{(-\dot{s})^{n-2m}}\right)^{\frac{1}{3(n-m-1)}} \lambda = \kappa_{\infty}^{-\frac{n-2m}{3(n-m-1)}} \tag{42}$$

for some positive constant κ_{∞}, so that

$$\Psi(\mu) \sim -\kappa_{\infty} \mu^{\frac{3(n-m-1)}{n-2m}} \quad \text{as} \quad \mu \to +\infty, \tag{43}$$

implying from (39) that the contact-line velocity is prescribed in this limit, independent of the thin film profile $h(x, t)$.

Given the matching condition (39) and the local results of [1], which imply in particular that $\epsilon = 0$ version of (32), *i.e.*,

$$\frac{\partial h}{\partial t} = -\frac{\partial}{\partial x}\left(h^n \left|\frac{\partial^3 h}{\partial x^3}\right|^{m-1} \frac{\partial^3 h}{\partial x^3}\right), \tag{44}$$

cannot have $\dot{s} < 0$ and cannot have $\dot{s} > 0$ with finite contact angle, we can now list the various scenarios which can arise in describing the macroscopic (outer) behaviour:

(a) (44) holds with $\dot{s}=0$, *i.e.*,

$$h=h^n\left|\frac{\partial^3 h}{\partial x^3}\right|^{m-1}\frac{\partial^3 h}{\partial x^3}=0 \quad \text{at } x=0. \tag{45}$$

(b) (44) holds with

$$h=h^n\left|\frac{\partial^3 h}{\partial x^3}\right|^{m-1}\frac{\partial^3 h}{\partial x^3}=0 \quad \text{at } x=s(t) \tag{46}$$

and

$$\frac{\mathrm{d}s}{\mathrm{d}t}=\epsilon^{\frac{n-2m-1}{n-2m}}\kappa_\infty\lambda^{\frac{3(n-m-1)}{n-2m}}, \tag{47}$$

corresponding to the limit (43) of (39). Since the solution to (44) will have local behaviour (40) as $z\to 0^-$, implying $\partial h/\partial x\to+\infty$, care must be taken in ensuring that this scenario is a self-consistent simplification of (39) in the limit $\epsilon\to 0$ (see below).

(c) The full conditions (46), (39) apply, but instead of the full balance (44) we have the quasi-steady one

$$\frac{\partial^2 h}{\partial x^2}=-p(t), \tag{48}$$

where p is the dimensionless pressure.

We now proceed to exploit each of these ingredients in piecing together the various possible regimes, taking $\lambda=O(1)$ in the first instance.

3.2. $t=O(1)$: FIXED FRONTS

In this section we describe the asymptotic behaviour of (32–33) as $\epsilon\to 0$ for $t=O(1)$. This can be regarded as an initial transient, the film profile subsequently evolving on a timescale having $t\gg 1$ as $\epsilon\to 0$, as described in Section 3.3. Here we need to make use of scenario (a). The leading-order solution is given by imposing (45) on (44), together with

$$h\to 1 \quad \text{as } x\to+\infty,$$
$$h=h_i(x) \quad \text{at } t=0.$$

In consequence, we have (for initial data h_i which decreases sufficiently rapid as $x\to 0^+$) local behaviour

$$h\sim a(t)x \quad \text{as } x\to 0^+ \tag{49}$$

for $2m+1<n<2m+2$ (which encompasses the case of shear-thickening fluids) and

$$h\sim D\left(\frac{x^{3m+1}}{t}\right)^{\frac{1}{n+m-1}} \quad \text{as } x\to 0^+ \tag{50}$$

for $n>2m+2$, where

$$D^{n+m-1}=\frac{1}{n+4m}\left(\frac{(m+n-1)^3}{(3m+1)(n-2m-2)(2n-m-3)}\right)^m. \tag{51}$$

In this latter case additional time scales need to be considered and we shall omit further discussion of this regime. In any case, the solution takes the self-similar form

$$h(x,t) \sim H_\infty\left(x \Big/ t^{\frac{1}{3m+1}}\right) \tag{52}$$

as $t \to \infty$, with

$$a(t) \sim A_\infty \Big/ t^{\frac{1}{3m+1}} \tag{53}$$

in (49) for some positive constant A_∞ which can be obtained numerically by solving the boundary-value problem for $H_\infty(\eta)$; when $h_i \equiv 1$ the asymptotic identities (37–39) become equalities.

For $2m+1 < n < 2m+2$, it follows from (39) that

$$s \sim -\epsilon^{\frac{n-2m-1}{n-2m}} \int_0^t \left(a(t')\right)^{\frac{3(n-m-1)}{n-2m}} \Psi\left(\lambda \Big/ a(t')\right) \mathrm{d}t' \tag{54}$$

for $\lambda = O(1)$, there being an inner region $x, h = O(\epsilon^{\frac{n-2m-1}{n-2m}})$ in which the leading-order problem is given by (48) with $p=0$, so that (matching with (49))

$$h \sim a(t)\,(x - s(t))\,. \tag{55}$$

From (43), (53) we thus have

$$s \sim \epsilon^{\frac{n-2m-1}{n-2m}} \kappa_\infty \lambda^{\frac{3(n-m-1)}{n-2m}} t \quad \text{as } t \to \infty \tag{56}$$

and when $h_i \equiv 1$

$$s \sim -\epsilon^{\frac{n-2m-1}{n-2m}} \kappa_0 A_\infty^{\frac{3(n-m-1)}{n-2m}} \frac{t^\beta}{\beta} \quad \text{as } t \to 0^+, \tag{57}$$

where $\beta = 1 + 3(n-m-1)/(n-2m)(3m+1)$, so that the interface reverses direction during this timescale (since $\Psi(\mu) \gtrless 0$ for $\mu \gtrless 1$, it follows that the interface initially moves to the left whenever $h_i'(0) > \lambda$, with discontinuous initial data corresponding to unbounded $h_i'(0)$).

3.3. $T = O(1)$: "FULL" BALANCE

3.3.1. *Formulation*

We now describe the ultimate behaviour of the film profile for (32–33). From (52) and (56) it is clear that the above separation of length scales becomes invalid for

$$t = \epsilon^{-\frac{(3m+1)(n-2m-1)}{3m(n-2m)}} T, \qquad x = \epsilon^{-\frac{n-2m-1}{3m(n-2m)}} X, \qquad s = \epsilon^{-\frac{n-2m-1}{3m(n-2m)}} S \tag{58}$$

with $T = O(1)$. Under these scalings the full balance holds in (44); moreover, since they imply that $\partial h/\partial x \to 0$ as $\epsilon \to 0$ for $h, X = O(1)$, we are justified in imposing the rescaled version of (47), *i.e.*,

$$\frac{\mathrm{d}S}{\mathrm{d}t} = \kappa_\infty \lambda^{\frac{3(n-m-1)}{n-2m}} \tag{59}$$

(*cf.* (56)) on the outer problem (whereby scenario (b) above pertains), even though the corresponding solution for h has infinite contact angle; this increase in slope is moderated over the inner problem (the suitably scaled version of (34–35) implied by (37)) which, in order to match, has far-field behaviour (40), thereby serving to select the contact-angle condition (59). The thin-film limit used in deriving (32) can itself remain self-consistent for similar reasons. Imposing (59) and (46) on (44) specifies the $T = O(1)$ problem, the small-T behaviour taking the form (52) (as expected by matching arguments).

3.3.2. *Large-time behaviour*

The large-time behaviour on this timescale cannot be governed by a travelling-wave balance in the full evolution equation because, unlike those of the shear-thinning case discussed above, such solutions cannot have an advancing interface at the 'front' $X = Q(T)$; this is in contrast to the 'back' $X = S(T)$, whose location is given by (59), with a local description of the form (40–41) applying in the evolution equation (in this case as $X - S \to 0^+$ rather than as $z \to \infty$). Instead a quasi-steady balance applies (*i.e.*, scenario (c) above holds) and we must first address the nature of the matching condition at $X = Q(T)$. Two outer regions are present, the 'hump' $S < X < Q$ and the 'undisturbed' region $X > Q$ in which

$$h \sim 1,$$

which acts as a prewetting layer (*cf.* [6]). There are also two inner regions, the first being an interior layer which is present at $X \sim Q$, whereby (again compare [6]) the dominant balance reads

$$\dot{Q}(h-1) = h^n \left| \frac{\partial^3 h}{\partial \hat{Z}^3} \right|^{m-1} \frac{\partial^3 h}{\partial \hat{Z}^3}, \tag{60}$$

where we have written $X = Q(T) + \hat{Z}$, subject to

$$\begin{aligned} &h \to 1 \quad \text{as } \hat{Z} \to +\infty, \\ &h \sim \Omega(T)\left(-\hat{Z}\right) \quad \text{as } \hat{Z} \to -\infty, \end{aligned} \tag{61}$$

where Ω must be determined as part of the solution to this boundary-value problem (which is uniquely specified up to translations in $\hat{Z}$), with scaling arguments implying that

$$\Omega(T) = \alpha \dot{Q}^{\frac{1}{3m}} \tag{62}$$

for some constant $\alpha(n, m)$ which can be determined numerically from (60–61).

As $T \to \infty$, the leading-order outer problem (which will prove to have scalings $h = O(T^{1/2})$, $Z = O(T^{1/2})$) therefore reads (now writing $X = S(T) + Z$, $S(T) \sim VT$ with the speed V given by (59) to have value $V = \kappa_\infty \lambda^{\frac{3(n-m-1)}{(n-2m)}}$)

$$\begin{aligned} &\frac{\partial^2 h}{\partial Z^2} = -P(T), \\ &h = 0 \text{ at } Z = 0, \\ &h = 0, \quad \frac{\partial h}{\partial Z} = -\alpha V^{\frac{1}{3m}} \quad \text{at } Z = Z_0(T), \end{aligned}$$

where $Q = VT + Z_0$ and, by leading-order conservation of mass,

$$\int_0^{Z_0} h(Z, T)\mathrm{d}Z = VT. \tag{63}$$

From this we readily obtain that

$$h = \frac{1}{2} P Z (Z_0 - Z), \qquad P = \left(\frac{2\alpha^3}{3}\right)^{\frac{1}{2}} V^{\frac{1-m}{2m}} T^{-\frac{1}{2}}, \qquad Z_0 = \left(\frac{6}{\alpha}\right)^{\frac{1}{2}} V^{\frac{3m-1}{6m}} T^{\frac{1}{2}}, \tag{64}$$

so for large T it follows that h takes the self-similar form

$$h \sim T^{\frac{1}{2}} \Theta\left(Z / T^{\frac{1}{2}}\right), \tag{65}$$

i.e., the rim thickness and height both grow as $T^{1/2}$. The scaling in the inner region in which (60) holds is $\hat{Z} = O(1)$, so the asymptotic structure just postulated is indeed self-consistent as $T \to \infty$. We note from (65) that the macroscopic contact angle is given asymptotically by $\Theta'(0)$, a constant.

To complete the description of the large-time behaviour, we note that (44) has a second inner region about $X = S(T)$, with $h = O(1)$, $Z = O(1)$ and leading-order balance

$$V = h^{n-1} \left| \frac{\partial^3 h}{\partial Z^3} \right|^{m-1} \frac{\partial^3 h}{\partial Z^3} \tag{66}$$

subject to local behaviour of the form (40) as $Z \to 0^+$ (corresponding to a single boundary condition on (66)) and, in order to match with (64), to

$$h \sim \tfrac{1}{2} P Z_0 Z \quad \text{as } Z \to +\infty \tag{67}$$

(corresponding to two boundary conditions, the slope $PZ_0/2$ being prescribed in this case).

The generalisation of the above results to the cylindrically symmetric case is again immediate, the various regions described above remaining one-dimensional to leading order.

3.4. Distinguished limit: $\lambda = O(\epsilon^{-1/3(1-m)})$

3.4.1. *One-dimensional solution*

In the section we discuss a scaling for the static contact angle which gives a fuller balance in the corresponding quasi-static formulation than that described above and we then address the stability of our one-dimensional solutions to perturbations in the transverse direction. We have deferred discussion of this case until now because the previous scaling $\lambda = O(1)$ is physically more natural, in particular since the slip term in (32) is then always negligible in the outer region. The current scaling does, however, lead to a fuller balance. Setting

$$\lambda = \epsilon^{-\frac{1}{3(1-m)}} \hat{\lambda} \tag{68}$$

(corresponding to λ large when $m < 1$, which includes the shear-thickening fluid case) and introducing the rescalings

$$x = \epsilon^{\frac{1}{3(1-m)}} \hat{x}, \qquad t = \epsilon^{\frac{3m+1}{3(1-m)}} \hat{t} \tag{69}$$

we obtain the full balance in (32), (33) for $\hat{t} = O(1)$ (for brevity we take $h_i(\hat{x})$ to be independent of ϵ here) and it remains only to discuss the large $\hat{t}$ asymptotics. Under the current scalings, with

$$s = \epsilon^{\frac{1}{3(1-m)}} \hat{s}, \qquad q = \epsilon^{\frac{1}{3(1-m)}} \hat{q}, \tag{70}$$

the conditions (39), (62) are now asymptotically valid as $\hat{t} \to \infty$, implying in that limit that

$$\frac{\partial^2 h}{\partial \hat{z}^2} = -\hat{p}\left(\hat{t}\right), \tag{71}$$

$$h = 0, \quad \frac{\mathrm{d}\hat{s}}{\mathrm{d}\hat{t}} = -\left(\frac{\partial h}{\partial \hat{z}}\right)^{\frac{3(n-m-1)}{n-2m}} \Psi\left(\hat{\lambda} / \frac{\partial h}{\partial \hat{z}}\right) \quad \text{at } \hat{z} = 0, \tag{72}$$

$$h = 0, \quad \frac{\partial h}{\partial \hat{z}} = -\alpha \left(\frac{\mathrm{d}\hat{q}}{\mathrm{d}\hat{t}}\right)^{\frac{1}{3m}} \quad \text{at } \hat{z} = \hat{z}_0(\hat{t}), \tag{73}$$

$$\int_0^{\hat{z}_0} h(\hat{z}, t) \mathrm{d}\hat{z} \sim \hat{s} \sim \hat{q}, \tag{74}$$

where $\hat{x}=\hat{s}(\hat{t})+\hat{z}$, gives the leading-order large-time problem, with solution

$$h=\tfrac{1}{2}\hat{p}\hat{z}\left(\hat{z}_0-\hat{z}\right), \quad \hat{s},\hat{q}\sim v\hat{t}. \tag{75}$$

It follows from (75) that $|\partial h/\partial\hat{z}|$ is the same at $\hat{z}=0$ and $\hat{z}=\hat{z}_0$, and hence the positive constant v in (75) is given by

$$v=-\left(\alpha^{3m}v\right)^{\frac{n-m-1}{m(n-2m)}}\Psi\left(\hat{\lambda}/\alpha v^{\frac{1}{3m}}\right), \tag{76}$$

requiring $\alpha v^{1/3m}>\hat{\lambda}$, so that $\Psi<0$. Moreover,

$$\hat{p}\sim\left(\frac{2\alpha^3}{3}\right)^{\frac{1}{2}}v^{\frac{1-m}{2m}}\hat{t}^{-\frac{1}{2}}, \qquad \hat{z}_0\sim\left(\frac{6}{\alpha}\right)^{\frac{1}{2}}v^{\frac{3m-1}{6m}}\hat{t}^{\frac{1}{2}}; \tag{77}$$

cf. (64). In contrast to (64), however, the wave speed v is here determined as part of the solution to the outer problem, rather than being selected *a priori* by the inner problem.

3.4.2. *Stability*

3.4.2.1. *Linear stability* We first note that the tendency to instability is a well-known feature of capillary ridges in other contexts. For brevity we neglect here the accumulation of mass due to the overrunning of the prewetting film; this simplification (which implies that the one-dimensional solution about which we perturb is a true travelling wave) is directly applicable over suitable timescales when a large initial hump is present and also applies more generally to the prewetted case when reinterpreted in an appropriate quasi-steady fashion. We thus replace (71–72) by (dropping $\hat{}$'s and generalising in the obvious way to two dimensions; we omit the asymptotic derivation of this generalisation, which itself represents an interesting class of moving-boundary problem related to the Hele-Shaw squeeze film formulation)

$$\begin{aligned}
&\nabla^2 h=-p(t)\\
&h=0, \quad \frac{\partial s}{\partial t}=\left(1+\left(\frac{\partial s}{\partial y}\right)^2\right)^{\frac{1}{2}}R\left(\left(1+\left(\frac{\partial s}{\partial y}\right)^2\right)^{-\frac{1}{2}}\left(\frac{\partial h}{\partial x}-\frac{\partial s}{\partial y}\frac{\partial h}{\partial y}\right)\right)\\
&\qquad\qquad\qquad\qquad\qquad\qquad\qquad\qquad \text{at } x=s(y,t),\\
&h=0, \quad \frac{\partial q}{\partial t}=\left(1+\left(\frac{\partial q}{\partial y}\right)^2\right)^{\frac{1}{2}}F\left(-\left(1+\left(\frac{\partial q}{\partial y}\right)^2\right)^{-\frac{1}{2}}\left(\frac{\partial h}{\partial x}-\frac{\partial q}{\partial y}\frac{\partial h}{\partial y}\right)\right)\\
&\qquad\qquad\qquad\qquad\qquad\qquad\qquad\qquad \text{at } x=q(y,t),
\end{aligned} \tag{78}$$

where, in the current context, the rear and front contact-line laws are given by

$$R(\Lambda)=-\Lambda^{\frac{3(n-m-1)}{n-2m}}\Psi\left(\lambda/\Lambda\right), \qquad F(\Lambda)=\alpha^{-3m}\Lambda^{3m}, \tag{79}$$

respectively. However, it is convenient, and of more general interest (for example when other regularisations apply), not to restrict ourselves to such special cases; pertinent properties in what follows are for $\Lambda\geq 0$ that $R'(\Lambda)\leq 0$ (for the limit discussed in Section 3.3 we have $R'(\Lambda)=0$), $F'(\Lambda)>0$, with $R(0)>0$ and $F(0)=0$, which ensures in particular that there is a single one-dimensional travelling-wave solution (up to translations in x), namely

$$\begin{aligned}
&p(t)=p_0, \qquad s_0(t)=vt, \qquad q_0(t)=vt+z_0,\\
&\quad x=vt+z, \qquad h_0(z,t)=\tfrac{1}{2}p_0 z(z_0-z)
\end{aligned} \tag{80}$$

with the constant contact angle given by $\Lambda = \Lambda^*$ where Λ^* is the unique positive root of

$$R(\Lambda^*) = F(\Lambda^*) \tag{81}$$

and with the constants p_0, v and z_0 then given by

$$v = R(\Lambda^*), \qquad z_0 = \left(\frac{6M}{\Lambda^*}\right)^{\frac{1}{2}}, \qquad p_0 = \left(\frac{2\Lambda^{*3}}{3M}\right)^{\frac{1}{2}}, \tag{82}$$

where

$$\int_0^{z_0} h_0(z')\mathrm{d}z' = M \tag{83}$$

gives the amount of fluid in a cross section. We note the wave speed v is independent of the mass M, a property not shared by the shear-thinning case (*cf.* (17)) and having important implications for what will follow.

We now perturb about this one-dimensional solution by setting (adopting a different notation from that in the previous subsection)

$$h = h_0 + H(z,y,t), \qquad s = s_0 + S(y,t), \qquad q = q_0 + Q(y,t), \qquad p = p_0 + P(t), \tag{84}$$

and linearise to give

$$\begin{aligned} &\nabla^2 H = -P, \\ &H + \Lambda^* S = 0, \qquad \frac{\partial S}{\partial t} = R'(\Lambda^*)\left(\frac{\partial H}{\partial z} - p_0 S\right) \quad \text{at } z = 0, \\ &H - \Lambda^* Q = 0, \qquad \frac{\partial Q}{\partial t} = -F'(\Lambda^*)\left(\frac{\partial H}{\partial z} - p_0 Q\right) \quad \text{at } z = z_0. \end{aligned} \tag{85}$$

Separating variables in the usual way, we set

$$\begin{aligned} &S(y,t) = S_0 \mathrm{e}^{\sigma t}\mathrm{e}^{\mathrm{i}ky}, \qquad Q(y,t) = Q_0 \mathrm{e}^{\sigma t}\mathrm{e}^{\mathrm{i}ky}, \\ &H(z,y,t) = \mathrm{e}^{\sigma t}\mathrm{e}^{\mathrm{i}ky}\left(A_+ \mathrm{e}^{kz} + A_- \mathrm{e}^{-kz}\right), \end{aligned} \tag{86}$$

the boundary conditions in (85) furnishing for $k \neq 0$

$$\begin{aligned} &A_+ + A_- + \Lambda^* S_0 = 0, \qquad \sigma S_0 = R'(\Lambda^*)\left(k(A_+ - A_-) - p_0 S_0\right), \\ &A_+ \mathrm{e}^{kz_0} + A_- \mathrm{e}^{-kz_0} - \Lambda^* Q_0 = 0, \qquad \sigma Q_0 = -F'(\Lambda^*)\left(k(A_+ \mathrm{e}^{kz_0} - A_- \mathrm{e}^{-kz_0}) - p_0 Q_0\right), \end{aligned}$$

yielding in turn the dispersion relation

$$\sigma^2 - \left(1 - \tfrac{1}{2}kz_0\coth(kz_0)\right)(\kappa_R + \kappa_F)\sigma + \left(1 + \tfrac{1}{4}k^2 z_0^2 - kz_0\coth(kz_0)\right)\kappa_R\kappa_F = 0 \tag{87}$$

for $\sigma(k)$, where $\kappa_R = -p_0 R'(\Lambda^*)$, $\kappa_F = p_0 F'(\Lambda^*)$ are non-negative. Hence

$$\begin{aligned} \sigma_\pm = \tfrac{1}{2}\Big\{ &\left(1 - \tfrac{1}{2}kz_0\coth(kz_0)\right)(\kappa_R + \kappa_F) \\ &\pm \left(\left(1 - \tfrac{1}{2}kz_0\coth(kz_0)\right)^2 (\kappa_R - \kappa_F)^2 + (kz_0\mathrm{cosech}(kz_0))^2 \kappa_R\kappa_F\right)^{\frac{1}{2}}\Big\}. \end{aligned}$$

For sufficiently large k the roots of (87) are both negative (provided $\kappa_R\kappa_F > 0$), with

$$\sigma \sim -\tfrac{1}{2}kz_0\kappa_R \quad \text{or} \quad \sigma \sim -\tfrac{1}{2}kz_0\kappa_F \quad \text{as } k \to \infty \tag{88}$$

giving linear stability for modes of large wave number. As $k \to 0$, however, we find that

$$\sigma_- \sim -\frac{k^2 z_0^2}{6}\frac{\kappa_R \kappa_F}{\kappa_R + \kappa_F}, \qquad \sigma_+ \sim \frac{1}{2}(\kappa_R + \kappa_F) - \frac{k^2 z_0^2}{6}\frac{(\kappa_R^2 + \kappa_R\kappa_F + \kappa_F^2)}{\kappa_R + \kappa_F}, \tag{89}$$

the former leading to decay for $\kappa > 0$ but the latter implying instability for sufficiently small wavenumbers. Indeed, we find from (87) that $\Re\mathrm{e}(\sigma_+)$ is monotonic decreasing with increasing k, crossing zero when

$$\tanh(kz_0) - \frac{4kz_0}{k^2 z_0^2 + 4} = 0 \tag{90}$$

is satisfied, *i.e.*, at $kz_0 \approx 2{\cdot}399$.

We note that the $k = 0$ solution gives (imposing conservation of mass)

$$H = \frac{1}{2}Pz(z_0 - z) + \frac{\Lambda^*}{z_0}(Q + S)z - \Lambda^* S, \qquad P = -\frac{3p_0}{z_0}(Q - S),$$

from which it follows (using the derivative boundary conditions in (85)) that, without loss of generality

$$S = -\kappa_R K_0 \mathrm{e}^{-(\kappa_R + \kappa_F)t}, \qquad Q = \kappa_F K_0 \mathrm{e}^{-(\kappa_R + \kappa_F)t} \tag{91}$$

for some constant K_0. The reason the exponential decay in (91) does not correspond to the exponential growth as $k \to 0$ implied by the second of (89) is clarified in the next section.

The one-dimensional solutions are thus linearly unstable, with long wavelengths exhibiting the fastest growth (in the radial case we thus anticipate that the instability will not manifest itself until the circumference of the contact line is, roughly speaking, large enough to fit in an unstable mode). This motivates a consideration of the limit in which variations with respect to y are slow and this we now pursue.

3.4.2.2. *The long-wavelength limit* Here we seek to shed some light onto the nonlinear evolution by taking the initial data to be slowly varying in y. Neglecting the y derivatives in (78) we have

$$h \sim \tfrac{1}{2}p(t)(q(y,t) - x)(x - s(y,t)) \tag{92}$$

with

$$\frac{\partial s}{\partial t} = R\left(\Lambda(y,t)\right), \qquad \frac{\partial q}{\partial t} = F\left(\Lambda(y,t)\right), \tag{93}$$

where

$$\Lambda(y,t) = \tfrac{1}{2}p(t)\Delta(y,t), \qquad \Delta(y,t) = q(y,t) - s(y,t). \tag{94}$$

The expressions (93–94) furnish four equations for s, q, Λ and Δ and thus represent a closed system if p is known; the mass in a cross-section at a given y is

$$M(y,t) = \frac{1}{12}p(t)\Delta^3(y,t) \tag{95}$$

and p is thus given by (assuming for simplicity that the problem is periodic in y, with (large) period L)

$$p(t) = \frac{12\bar{M}}{\bar{\Delta}^3(t)} \tag{96}$$

where the overbar denotes the relevant average, *i.e.*,

$$\bar{\Phi}(t) = \frac{1}{L}\int_0^L \Phi(y,t)\mathrm{d}y, \tag{97}$$

so that $\bar{M}$ is a known constant (given by overall conservation of mass). Finally, (93–94) imply that

$$\frac{\partial \Delta}{\partial t} = \Omega\left(\tfrac{1}{2}p\Delta\right), \tag{98}$$

where

$$\Omega(\Lambda) = F(\Lambda) - R(\Lambda). \tag{99}$$

Equations (96–98) provide our (non-local) governing system for Δ and p.

As noted in the previous subsection, (89) implies $\sigma_+ > 0$ for $k = 0$, which might seem to suggest that even in one dimension the travelling wave is unstable and indeed, suppressing the y-dependence, it follows from (98) and $\Omega'(\Lambda) > 0$ that if we (erroneously) regard p as prescribed then the solution corresponding to (81) is unstable; this is misleading, however, because of the non-local aspect of (96–98) which yields in the one-dimensional case that

$$\frac{\mathrm{d}\Delta}{\mathrm{d}t} = \Omega\left(\frac{6M}{\Delta^2}\right), \tag{100}$$

which implies stability and is consistent with (91). The fact that p is determined in (78) by a non-local constraint thus has important implications. In higher dimensions (96–98) is of course unstable to y-dependent perturbations, suggesting the ridge of fluid will seek to break up into droplets. Indeed, for the constraints on F and R noted above we have that

$$\frac{\partial \Delta}{\partial t} \sim -R(0) \quad \text{as} \quad \Delta \to 0$$

so such break-up will occur within the current limit problem in some finite time, with (generically)

$$\Delta \sim R(0)(t_c - t) + \Delta_c(y - y_c)^2$$

close to the break up time $t = t_c$ and location $y = y_c$, for some positive constant Δ_c. Nevertheless, this long-wavelength instability is (at least in its initial stages) a relatively innocuous one, with the slowly-varying approximation (and the time-dependence implied by the one-dimensional solution) remaining valid until attempted break-up of this type occurs (the $\epsilon \to 0$ analysis above of course ceases to apply when Δ becomes sufficiently small with respect to ϵ; the ultimate behaviour after such breakdown occurs remains open). The instability mechanism can be described as follows. Were the pressure allowed to vary in such a way that the film in each cross-section (*i.e.*, for each y) was able to approach equilibrium, requiring $p = 2\Lambda^*/\Delta$, then p would be largest in regions of small Δ; this pressure difference would drive fluid into the regions of larger Δ, implying that the rim has a tendency to become thinner where it is already thinnest, allowing the pressure, which is responsible for the non-local nature of the problem, to remain uniform, as it in fact needs to be.

The corresponding stability issues would also be worth addressing in the shear-thinning case, though here the base solution for the linear stability problem (that described in Section 2) is significantly more complex than in the shear-thickening case, so while the problem is straightforward to formulate its solution is not immediate. We shall not pursue such matters

here, though we note that the problem is again made clearer by using the travelling wave (having finite contact angle at the dewetting interface and zero contact angle at its front) as the base solution, rather than the solution of Section 2 (which itself has non-trivial time dependence because of the accumulation of mass within the rim).

4. Newtonian fluids; $m=1$, $n=3$

The borderline case $n=2m+1$ is naturally the most delicate. Here we shall limit our discussion to the Newtonian case $m=1$, $n=3$ in view of its obvious physical significance. For brevity we present the asymptotic derivation in a somewhat *ad hoc* manner; we stress that it can be made fully systematic. For experimental results with which the resulting rim profiles can be compared, see [33] for example.

The initial formulation is given in (32–33) and the inner problem at $x=s$ is governed by (34–35) (in each case with $m=1$, $n=3$); the constraint (36) can no longer be imposed, however. Setting

$$h=\epsilon\Phi(\lambda z/\epsilon, t),$$

and taking $\lambda=O(1)$ we have that $\Phi(\xi,t)$ satisfies at leading order

$$\Phi(\Phi+1)\frac{\partial^3\Phi}{\partial\xi^3}=\frac{\dot{s}}{\lambda^3}, \tag{101}$$
$$\Phi=0, \quad \frac{\partial\Phi}{\partial\xi}=1 \quad \text{at } \xi=0.$$

The evolution is slow for small ϵ, *i.e.*, $|\dot{s}|\ll 1$, and to leading order (101) then implies for $\xi=O(1)$ that

$$\Phi\sim\xi, \tag{102}$$

the asymptotic structure of (101) with $|\dot{s}|\ll 1$ subdivides into two regions, however, the second having

$$\Phi\sim\xi\phi(\zeta), \quad \zeta=\dot{s}\log\xi$$

with leading-order balance

$$\phi^2\frac{\mathrm{d}\phi}{\mathrm{d}\zeta}=-\frac{1}{\lambda^3}$$

so that, on matching with (102),

$$\frac{1}{3}\phi^3=\frac{1}{3}-\frac{1}{\lambda^3}\zeta. \tag{103}$$

The outer region corresponds to the scale $z=O(\Delta)$, so that $\zeta\sim\dot{s}\log(\Delta/\epsilon)$. From (103) we thus obtain the matching condition

$$\frac{\partial h}{\partial x}=\lambda\left(1-\frac{3}{\lambda^3}\log(\Delta/\epsilon)\dot{s}\right)^{\frac{1}{3}} \quad \text{at} \quad x=s(t) \tag{104}$$

on the outer solution, the right-hand side of (104) representing the "macroscopic" contact angle.

We again locate the "front" at $x=q(t)$, with $\Delta(t)=q(t)-s(t)$, and set $x=q(t)+\hat{z}$ to give (*cf.* [28], for example)

$$h-1=h^3\frac{\mathrm{d}^3h}{\mathrm{d}\hat{\zeta}^3}$$

at leading order, where $\hat{\zeta}=\dot{q}^{\frac{1}{3}}\hat{z}$, subject to

$$\begin{aligned} &h\to 1 \quad \text{as} \quad \hat{\zeta}\to+\infty,\\ &h\sim\left(3\log(-\hat{\zeta})\right)^{\frac{1}{3}}(-\hat{\zeta}) \quad \text{as} \quad \hat{\zeta}\to-\infty. \end{aligned} \tag{105}$$

Since $-\hat{z}=O(\Delta)$ corresponds to $\log(-\hat{\zeta})\sim\log(\Delta^3\dot{q})/3$, (105) yields the matching condition

$$\frac{\partial h}{\partial x}=\left(\log(\Delta^3\dot{q})\dot{q}\right)^{\frac{1}{3}} \quad \text{at} \quad x=q(t) \tag{106}$$

on the outer solution. Since $q\sim s$, $\Delta\ll s$ applies for large time, we have quasi-steady outer solution

$$h\sim\frac{6s}{\Delta^3}z(\Delta-z), \tag{107}$$

so that conditions (104) and (106) read

$$\frac{6s}{\Delta^2}\sim\lambda\left(1-\frac{3}{\lambda^3}\log(\Delta/\epsilon)\dot{s}\right)^{\frac{1}{3}}\sim\left(\log(\Delta^3\dot{s})\dot{s}\right)^{\frac{1}{3}}. \tag{108}$$

Rearranging the second and third of (108) we have

$$\log(\Delta^6\dot{s}/\epsilon^3)\dot{s}\sim\lambda^3. \tag{109}$$

The appropriate way to balance in (108–109) is to set

$$s(t)=\frac{t}{\log(1/\epsilon)}S(\tau), \quad \Delta(t)=\frac{t^{\frac{1}{2}}}{\log^{\frac{1}{2}}(1/\epsilon)}\delta(\tau), \quad \tau=\frac{\log t}{\log(1/\epsilon)}, \tag{110}$$

and thus to obtain for $\tau=O(1)$ with $\tau>0$ that

$$3(1+\tau)S\sim\lambda^3, \quad 6S/\delta^2\sim(3\tau S/2)^{\frac{1}{3}}$$

i.e.,

$$S\sim\frac{\lambda^3}{3(1+\tau)}, \quad \delta\sim\frac{2^{\frac{2}{3}}\lambda}{\tau^{\frac{1}{6}}(1+\tau)^{\frac{1}{3}}}; \tag{111}$$

note that the $\dot{s}$ term inside the logarithm in the last expression (108) does not feature in the leading-order balance and can thus be deleted there. From (107), the macroscopic contact angle (*i.e.*, the gradient of the outer solution at $z=0$) $\sim 2^{1/3}\lambda\tau^{1/3}/(1+\tau)^{1/3}$, and thus asymptotes to a value $2^{1/3}$ larger than the microscopic one λ. We observe from (110) that the basic time dependence is as for the shear-thickening case, but there are logarithmic corrections to the power-law dependence (as is typical for a borderline exponent). Experimental data is often classified according to the power-law exponent γ in $s\propto t^{\gamma}$ as $t\to\infty$; defining $\gamma(t)$ via

$$\gamma(t)=t\dot{s}/s, \tag{112}$$

it follows from (110) that

$$\gamma \sim 1 + \frac{1}{\log(1/\epsilon)} \frac{1}{S} \frac{\mathrm{d}S}{\mathrm{d}\tau}$$

so that, by (111),

$$\gamma \sim 1 - \frac{1}{\log(1/\epsilon)} \frac{1}{(1+\tau)} = 1 - \frac{1}{\log(t/\epsilon)}, \tag{113}$$

the correction terms omitted in (113) are of course only logarithmically smaller in ϵ than those included. We observe from (113) that the exponent γ asymptotes to unity as $t \to \infty$ but the limit is approached very slowly (but monotonically over the relevant timescales), so over intermediate timescales significantly smaller values can be expected to be observed; behaviour of this type is indeed observed in practice (*cf.* [34] and [13]).

We note that, while we have used the Navier-slip regularisation to allow contact line motion, in the Newtonian case the results have certain universal properties (*cf.* [4] for the wetting case) which do not depend on the choice of regularisation. This is not, however, the case for shear-thickening fluids [6]; moreover, even in the Newtonian case the logarithmic terms in (104), (106) do depend on the regularisation (though the dominant (*i.e.*, algebraic in t) time dependence, as reflected by (110), does not).

For consistency with Section 4, we need finally to note two other aspects of the analysis; we shall not go into detail in this borderline case, however. Firstly, there is a shorter time scale with (for $\lambda = O(1)$) scalings, $t = O(\log^{4/3}(1/\epsilon))$ scalings, $x = O(\log^{1/3}(1/\epsilon))$ on which the full evolution equation holds in the outer region and the hump first emerges. Secondly, stability matters can readily be pursued in higher dimensions. In the constant mass case (*i.e.*, non-prewetting) the first expression in (108) becomes $6M/\Delta^2$ for constant M, so we obtain a true travelling wave ($\dot{s}$, Δ constant) and the analysis goes through essentially as in Section 3.4.2. For the prewetted case there is in effect a multiple-scales problem, the timescale on which slow modulations occur corresponding to τ above, though instabilities will in any case manifest themselves before such subtleties come into play.

5. Discussion

We start by summarising the results for the distinct regimes of shear-thinning and shear-thickening fluids arising in describing the large-time behaviour. In the former case, the key time and parameter dependencies are embodied in (18), with the "rim" profile being given by a full travelling-wave balance within the evolution equation (here the local behaviour at the contact line is innocuous but the outer solution non-trivial). The converse occurs for shear-thickening fluids, whereby (65) describes the time dependence in the rim, whose profile takes the simple quasi-steady form (64); in this case, however, the contact-line inner problem is highly non-trivial and plays a dominate role in determining the (constant) contact-line velocity V. Thus different contact-line physics (or, equivalently, different choices of regularisation) lead to quite different (but constant) contact-line velocities, but the time dependence (65) remains valid. The borderline, Newtonian, case has universal properties because (*cf.* [4]) it is neither outer or inner driven, but the logarithmic modulations of the basic time dependence (as described in Section 4) are sensitive to the choice of regularisation. We have also investigated certain stability issues, for which the adoption of a quasi-steady approximation requires that the corresponding frequencies not be too high; we refer to [35] for a discussion (in a somewhat different context) of why higher frequencies can be expected to be damped.

More, precisely, the time dependence as large times (for one-dimensional or radially-symmetric solutions to (1)) can be characterised for power-law fluids ($n=m+2$) but the exponents γ_s, γ_Δ and γ_h in the contact-line location, $s \propto t^{\gamma_s}$, the rim thickness, $\Delta \propto t^{\gamma_\Delta}$, and height, $h_{\max} \propto t^{\gamma_h}$ (in each case as $t \to \infty$), as follows. Conservation of mass requires that $\gamma_s = \gamma_\Delta + \gamma_h$ and for shear-thinning fluids ($m > 1$) we have (see (18)) $\gamma_s = 2/(m+1)$, $\gamma_\Delta = 1/(m+1)$, $\gamma_h = 1/(m+1)$, while for shear-thickening ones ($0 < m < 1$) we have (see (64)) $\gamma_s = 1$, $\gamma_\Delta = 1/2$, $\gamma_h = 1/2$. Finally, in the borderline (Newtonian) case $m = 1$ it follows from (110–111) that $s \propto t/\log t$, $\Delta \propto t^{1/2}/\log^{1/2} t$, $h_{\max} \propto t^{1/2}/\log^{1/2} t$.

A number of generalisations are possible, notably to (unscaled) contact angles which are not small, so that the "rim" profiles are governed by full slow-flow problems rather than their lubrication limits. The large-time behaviour remains analytically tractable in the shear-thickening and Newtonian cases, the (capillary quasi-static) parabolic profile (as in Equation (64)) being replaced by a cylindrical cap. In the shear-thinning case, a (quasi-steady) travelling wave reduction of the full system will provide the relevant profile and would represent a worthwhile free-boundary problem in its own right. Such "thick-film" versions of the problem would also be physically relevant to the corresponding flows of power-law or Newtonian fluids in a Hele-Shaw cell, their thin-film limit being encompassed by (2) with, [1], $n = 1$. In this Hele-Shaw case the flow can again be over a planar substrate or the substrate can be replaced by a symmetry boundary (in which case a $\pi/2$ contact-angle, and hence a "thick-film" formulation, necessarily applies); in the unconfined Stokes flow case the symmetric problem of course has a quite different thin-film limit from (2) and has been the subject of extensive analysis in its own right (with the same formulation also describing the case in which a zero shear stress, rather than a no slip, condition is imposed between the fluid film and the substrate; *cf.* [36], for example, and references therein for related considerations).

Other generalisations would be to initial data which, say, grow or decay as x^q for all x for some exponent $q \neq 0$. For $q = 1$ (a wedge of fluid) the solution for a shear-thinning fluid of fixed contact angle is given for all time by the relevant similarity reduction (in both thin- (small wedge angle) and thick-film versions of the formulation). For $q > 1$ the small-time behaviour involves a hump near to the origin, of the type described above, while wetting (*i.e.*, $\dot{s} < 0$) occurs for large-time, the leading-order outer problem seeing a zero contact angle at the interface; the reverse is true for $q < 1$, the approach above then being applicable to the large-time behaviour. Related higher-dimensional problems with initial data in the form of a cone of fluid, say, are also readily formulated.

Finally, we note that when gravitational effects are non-negligible (*cf.* [37] and [38] for example, for the Newtonian case) additional phenomena come into play, providing other directions in which the analysis could be generalised.

Acknowledgements

We gratefully acknowledge the financial support of the EPSRC. We are also grateful to the referees for a number of helpful comments and additional references.

References

1. J. R. King, Two generalisations of the thin film equation. *Math. Comp. Mod.* 34 (2001) 737–756.
2. L. M. Hocking, Rival contact-angle models and the spreading of drops. *J. Fluid Mech.* 239 (1992) 671–681.
3. Y. D. Shikhmurzaev, Moving contact lines in liquid/liquid/solid systems. *J. Fluid Mech.* 334 (1997) 211–249.
4. J. R. King, Thin-film flows and high-order degenerate parabolic equations. In: A. C. King and

Y. D. Shikhmurzaev (eds.), *Proc. of the IUTAM Symposium on Free Surface flows*, Dordrecht: Kluwer (2001) pp. 7–18.
5. D. E. Weidner and L. W. Schwartz, Contact-line motion of shear-thinning liquids. *Phys. Fluids* 6 (1994) 3535–3538.
6. J. R. King, 2001. The spreading of power-law fluids. In: A. C. King and Y. D. Shikhmurzaev (eds.) *Proc. of the IUTAM Symposium on Free Surface flows*, Dordrecht: Kluwer (2001) pp. 153–160.
7. L. Ansini and L. Giacomelli, Shear-thinning liquid films: macroscopic and asymptotic behaviour of quasi-self-similar solutions. *Nonlinearity* 15 (2002) 2147–2164.
8. V. M. Starov, A. N. Tyatyushkin, M. G. Velarde and S. A. Zhdanov, Spreading of non-Newtonian liquids over solid substrates. *J. Coll. Interf. Sci.* 257 (2003) 284–290.
9. S. K. Wilson, B. R. Duffy and R. Hunt, A slender rivulet of a power law fluid driven by either gravity or a constant shear stress at a free surface. *Q. J. Mech. Appl. Math.* 55 (2002) 385–408.
10. F. Saulnier, E. Raphael and P.-G. de Gennes, Dewetting of thin-film polymers. *Phys. Rev. E* 66 (2002) art: 061607.
11. K. Jacobs, R. Seemann, G. Schatz and S. Herminghaus, Growth of holes in liquid films with partial slippage. *Langmuir* 14 (1998) 4961–4963.
12. A. Carre and F. Eustache, Spreading kinetics of shear-thinning fluids in wetting and dewetting modes. *Langmuir* 16 (2000) 2936–2941.
13. A. Ghatak, R. Khanna, and A. Sharma, Dynamics and morphology of holes in dewetting of thin films. *J. Coll. Interf. Sci.* 212 (1999) 483–494.
14. A. L. Bertozzi, G. Grun and T. P. Witelski, Dewetting films: bifurcation and concentrations. *Nonlinearity* 14 (2001) 1569–1592.
15. L. W. Schwartz, R. V. Roy, R. R. Eley and S. Petrash, Dewetting patterns in a drying liquid film. *J. Coll. Interf. Sci.* 14 (2001) 363–374.
16. R. Limary and P. F. Green, Dewetting instabilities in thin block copolymer films: nucleation and growth. *Langmuir* 15 (1999) 5617–5622.
17. K. R. Shull and T. E. Karis, Dewetting dynamics for large equilibrium contact angles. *Langmuir* 10 (1994) 334–339.
18. C. Redon, F. Brochard-Wyart and F. Rondelez, Dynamics of dewetting. *Phys. Rev. Lett.* 66 (1991) 715–718.
19. A. Buguin, L. Vovelle and F. Brochard-Wyatt, Shocks in inertial dewetting. *Phys. Rev. Lett.* 83 (1999) 1183–1186.
20. G. Reiter, Dewetting of thin polymer films. *Phys. Rev. Lett.* 68 (1992) 75–78.
21. R. Khanna and A. Sharma, Pattern formation in spontaneous dewetting of thin apolar films.*J. Coll. Interf. Sci.* 195 (1997) 42–50.
22. F. S. Merkt, R. D. Deegan, D. I. Goldman, E. C. Rericha and H. L. Swinney, Persistent holes in a fluid. Preprint.
23. G. Reiter and A. Sharma, Auto-optimisation of dewetting rates by rim instabilities in slipping polymer films. *Phys. Rev. Lett.* 87 (2001) art: 166103.
24. I. W. Hamley, E. L. Hiscutt, Y. -W. Yang and C. Booth, Dewetting of thin block copolymer film. *J. Coll. Interf. Sci.* 209 (1999) 255–260.
25. P. L. Evans, L. W. Schwartz and R. V. Roy, A mathematical model for crater defect formation in a drying paint layer. *J. Coll. Interf. Sci.* 227 (2000) 191–205.
26. F. Brochard-Wyart, P. -G. Degennes, H. Hervert and C. Redon, Wetting and slippage of polymer melts on semi-ideal surfaces. *Langmuir* 10 (1994) 1566–1572.
27. G. Reiter and R. Khanna, Kinetics of autophobic dewetting of polymer films. *Langmuir* 16 (2000) 6351–6357.
28. J. R. King and M. Bowen, Moving boundary problems and non-uniqueness for the thin film equation. *Euro. J. Appl. Math.* 12 (2001) 321–356.
29. K. Kargupta and A. Sharma, Creation of ordered patterns by dewetting of thin films on homogeneous and heterogeneous substrates. *J. Coll. Interf. Sci.* 245 (2002) 99–115.
30. S. Herminghaus, R. Seemann and K. Jacobs, Generic morphologies of viscoelastic dewetting fronts. *Phys. Rev. Lett.* 89 (2002) art: 056101.
31. T. P. Witelski and A. J. Bernoff, Stability of self-similar solutions for van der Waals driven thin film rupture. *Phys. Fluids* 11 (1999) 2443–2445.
32. W. W. Zhang and J. R. Lister, Similarity solutions for van der Waals rupture of a thin film on a solid substrate. *Phys. Fluids* 11 (1999) 2454–2462.

33. R. Seeman, S. Herminghaus and K. Jacobs, Shape of a liquid front upon dewetting. *Phys. Rev. Lett.* 87 (2001) art: 196101.
34. G. Reiter, P. Auroy and l. Auvray, Instability of thin polymer films on layers of chemically identical grafted molecules. *Macromolecules* 29 (1996) 2150–2157.
35. B. S. Tilley, S. H. Davis and S. G. Bankoff, Unsteady Stokes flow near an oscillating, heated contact line. *J. Fluid Mech.* 438 (2001) 339–362.
36. F. Saulnier, E. Raphael and P.-G. de Gennes, Dewetting of thin polymer films near the glass transition. *Phys. Rev. Lett.* 88 (2002) art: 196101.
37. J. A. Moriarty and L. W. Schwartz, Dynamics considerations in the closing and opening of holes in thin liquid films. *J. Coll. Interf. Sci.* 161 (1993) 335–342.
38. P. G. López, M. J. Mikis and S. G. Bankoff, Stability and evolution of a dry spot. *Phys. Fluids* 13 (2001) 1601–1614.